2009

In situ element quantification in the hydrothermal diamond anvil cell using synchrotron x-ray fluorescence with applications toward subduction zone processes

Steven Joseph Maglio
University of Nevada Las Vegas

IN SITU ELEMENT QUANTIFICATION IN THE HYDROTHERMAL DIAMOND ANVIL CELL USING SYNCHROTRON X-RAY FLUORESCENCE WITH APPLICATIONS TOWARD SUBDUCTION ZONE PROCESSES

by

Steven Joseph Maglio

Bachelor of Science
Northern Illinois University
2005

Master of Science
Northern Illinois University
2007

A thesis submitted in partial fulfillment of
the requirements for the

Master of Science in Geoscience
Department of Geoscience
College of Sciences

Graduate College
University of Nevada, Las Vegas
December 2009

UNLV
UNIVERSITY OF NEVADA LAS VEGAS

THE GRADUATE COLLEGE

We recommend that the thesis prepared under our supervision by

Steven Joseph Maglio

entitled

In Situ Element Quantification in the Hydrothermal Diamond Anvil Cell Using Synchrotron X-Ray Fluorescence with Applications toward Subduction Zone Processes

be accepted in partial fulfillment of the requirements for the degree of

Master of Science
Geoscience

Adam Simon, Committee Chair

Oliver Tschauner, Committee Member

Eugene Smith, Committee Member

Andrew Cornelius, Graduate Faculty Representative

Ronald Smith, Ph. D., Vice President for Research and Graduate Studies
and Dean of the Graduate College

December 2009

ABSTRACT

In situ Element Quantification in the Hydrothermal Diamond Anvil Cell Using Synchrotron X-ray Fluorescence with Applications Toward Subduction Zone Processes

by

Steven Joseph Maglio

Dr. Adam Simon, Examination Committee Chair
Assistant Professor of Geoscience
University of Nevada, Las Vegas

Yttrium is used in geochemical investigations of arc volcanics and metamorphic geothermometers. The ability to use Y as a geochemical tool is predicated on an understanding of the mobility of Y during fluid-saturated conditions attending metamorphic and igneous processes. The goal of this work was to use the hydrothermal diamond anvil cell (HDAC) and synchrotron radiation X-ray fluorescence to quantify, in situ, the concentration of Y in aqueous fluids at 2-5 GPa and 650 – 800 °C; conditions likely at the oceanic lithosphere - mantle wedge interface in subduction zones. Previous studies have used modified diamond anvils which limits their maximum pressure to ~2 GPa. I used unmodified diamond anvils to extend this range to greater pressure, hence simulating greater depth (about 80-140 km), where significant dehydration of the subducting oceanic lithosphere is hypothesized to occur. With the detectors oriented 10° relative to forward scattering geometry, Rayleigh scattering of the diamond anvils was sufficiently reduced to observe Y fluorescence within the HDAC. However, I observed a non-linear relationship between concentration and fluorescence. The new technique offers great promise, and future work to increase sensitivity, perhaps by increasing counting times, is warranted.

ACKNOWLEDGEMENTS

The author would like to acknowledge the contributions to this work by his advisor, Adam Simon, and co-advisor, Oliver Tschauner, and reviews from Eugene Smith and Andrew Cornelius. Also of importance was the feedback and loan of supplies from Mark Frank as well as the help of the HPCAT staff (Yuming Xiao, Paul Chow, Guoyin Shen, Eric Rod), UNLV Physics machinists Jim Norton and Amo Sanchez, Professor John Hanchar of Memorial University Newfoundland, and Dr. David Schiferl, LANL, for help and feedback along the course of these investigations. We gratefully acknowledge support from the U.S. Department of Energy Cooperative Agreement Nos. DE-FC08-01NV14049 and DE-FC8806NA27684 with the University of Nevada Las Vegas. Additional, partial support was provided by internal scholarships from the Geoscience Department, University of Nevada, Las Vegas. This work was performed at HPCAT (Sector 16), Advanced Photon Source (APS), Argonne National Laboratory. HPCAT is supported by DOE-BES, DOE-NNSA, NSF, and the W.M. Keck Foundation. APS is supported by DOE-BES, under Contract No. DE-AC02-06CH11357.

TABLE OF CONTENTS

LIST OF FIGURES

CHAPTER 1

INTRODUCTION

Incompatible trace elements, such as the high field strength elements (HFSE), large ion lithophile elements (LILE), and rare earth elements (REE), can be used as tracers of geochemical processes that occur at the interface between subducting oceanic lithosphere and stratigraphically overlying mantle wedge (cf., Sun and McDonough, 1989, Elliot, 2003, Manning, 2004). Aqueous fluids that are released during dehydration reactions in subducting oceanic plates transport incompatible trace elements into the mantle wedge and/or induce melting in the mantle wedge that may also scavenge incompatible trace elements from the subducting oceanic plate (Ayers and Watson, 1991, Hawkesworth et al., 1993, Iwamori, 1998, 2004, Plank and Langmuir, 1998, Schmidt and Poli, 1998, Reed et al., 2000, Manning, 2004, Grove et al., 2006, Kawamoto, 2006, Spandler et al., 2007, Zack and John, 2007). Quantitative constraints on the mass transfer of incompatible trace elements, specifically those used as tracers of geochemical processes, between minerals and fluids, either aqueous or silicate or both, are critical to developing a better understanding of the links between the subduction process and arc volcanism (Figure 1).

Yttrium, although of less mass than the lanthanides, is often grouped with them and considered a rare earth element (REE), as the lanthanides are often referred. While not as prominent in trace element geochemistry as other REE, yttrium is important in a number of geochemical analyses. Lithium isotopes and the Li/Y ratio of arc volcanic rocks have been hypothesized to represent the addition of aqueous fluid to the mantle wedge across a volcanic arc (Moriguti and Nakamura, 1991, Chan et al., 1999). Additionally, the relationship between the Y concentration and the ratio of Sr/Y in arc volcanics may be an

analog to the amount of melt generated in the sub-arc mantle wedge due to the addition of aqueous fluid from the subducted oceanic plate (Ewart et al., 1998). Further, generation of adakite magmas, originally described by Kay (1978), which are hypothesized to be the result of melting of the subducting oceanic plate, are characterized by high Sr/Y, La/Yb ratios and low Y, Yb, and high field strength element (HFSE; Zr, Nb, Ta, REE) concentrations (i.e., Beate et al., 2001).

It is clear, given these previous studies, that knowledge of how Y behaves in the presence of aqueous fluids and solid matter (rock) is germane to understanding the processes occurring in subduction zone environments. It would be ideal to recreate the fluids generated during dehydration of a subducting oceanic plate (to their closest hypothesized compositions), but we have elected to use a much simpler fluid ($H_2O \pm HNO_3$) to achieve a baseline with which to compare future experimental results.

The aqueous fluid phase may be the medium by which mass is transferred from ocean lithosphere to the mantle wedge and yet most of the available experimental techniques offer only an indirect constraint on the fluid solute load at pressure (P) and temperature (T). Rather, most previous attempts to constrain element mobility in a fluid-saturated assemblage at the P and T conditions attending devolatilization and melting at the base of arc volcano plumbing systems have relied upon a mass balance approach wherein the elemental composition of each phase is quantified before and after the experiment (e.g., Keppler, 1996, Johnson and Plank, 1999, Klemme et al., 2005, Plank, 2005, Prowatke and Klemme, 2006, Hermann and Spandler, 2008). Such experiments have been performed by using piston-cylinder or multi-anvil apparatuses, and pre- and post-run

assemblage materials were analyzed by using electron probe microanalysis (EPMA) and/or laser ablation-inductively coupled plasma-mass spectrometry (LA-ICP-MS).

Controversy has plagued these recovery techniques owing: 1) to the lack of precision in quantifying trace element abundances in all phases, 2) whether or not trace element equilibrium was achieved, and 3) whether quench reactions modify the trace element chemistry of recovered phases. Kessel et al. (2004, 2005) overcame these experimental challenges by trapping all run products, solids and fluid, in a modified diamond trap assemblage (Baker and Stolper, 1994), and analyzing all run products with LA-ICP-MS. More recently, experimentalists have used the hydrothermal diamond anvil cell (HDAC) and synchrotron X-ray fluorescence (SXRF) to quantify the concentration of trace elements in aqueous fluid at elevated P and T (cf., Sanchez-Valle et al., 2003, Schmidt et al., 2007; Manning et al., 2008; Sibert et al., 2008). However, there are significant challenges when using the HDAC that previous studies have not overcome. These are: 1) parasitic fluorescence of the solid phase from low intensity X-ray beam "tails" that have not been properly blocked/removed; 2) the accuracy of calibration of peak area to concentration as the relationship may not be linear; and, 3) an experimental setup that does not require modification of the diamond anvils and/or HDAC, i.e., drilling perforations or recesses in the diamonds which limits the experiments to pressures no greater than 2 GPa. If there is any possibility of parasitic fluorescence during the experiment, the recorded peak areas may have a contribution from the fluorescence of the solid phase. Thus, the data would not be representative solely of the concentration of the trace elements in the fluid.

Previous experimental studies (Sanchez-Valle et al., 2003; Manning et al., 2008) have used single points for the calibration of peak area to concentration (i.e., using a single known concentration relative to the experimental value). If, and this is may be likely, the peak area to concentration relationship is not linear, the previous experiments may need to be reevaluated with more complete calibration curves. Sanchez-Valle et al. (2003) used an experimental setup similar to that attempted here where little modification of the diamond anvils and/or HDAC was required. This preserves the HDAC for a variety of future techniques and does not otherwise limit the pressure range attainable with the HDAC. Schmidt et al. (2007), Manning et al. (2008), and Sibert et al. (2008) used techniques where the diamonds were modified to permit fluorescence measurements in ninety degree geometry. This eliminates the possibility of parasitic fluorescence, but limits pressures to ≤ 2 GPa because the modified (i.e., perforated, drilled, plates instead of anvils, or otherwise altered) diamond anvils have significantly reduced strength. The current study was designed to extend the pressure range of the *in situ* HDAC technique wherein the concentration of trace elements in aqueous fluid could be quantified while the sample is held at P and T between 2–5 GPa and 600–850 °C, respectively. These P-T conditions are relevant to the interface between the sub-arc mantle wedge and subducting oceanic lithosphere. The envisioned technique would bypass quench-modification complications by quantifying directly the concentration of trace elements in the fluid phase. These data would expand significantly our understanding of element mass transfer at the base of the arc volcanic plumbing system.

CHAPTER 2

METHODS

Experimental Design

The Bassett-type HDAC (Bassett et al., 1993; Bassett, 2003) was used during these experiments (Figure 2). Readers are referred to Bassett et al. (1993) and Bassett (2003) for detailed schematics of the HDAC configuration. The diamond anvils were obtained from Foxwood Instruments, had 650-micrometer culets, and were approximately 1.8 millimeters in length from the table to the culet. The gasket material was inconel with an original thickness of 250 micrometers. Each gasket was pre-indented (reducing the thickness to 70-90 micrometers) by increasing the pressure of the diamond anvils on the gasket. Increasing pressure was achieved by turning 3 bolts that thread into the HDAC. The sample chamber was created by using a Hylozoic Products Micro Electric Discharge Machine (EDM) to "drill" holes of approximately 300 micrometers in the center of the compressed region of the gasket.

Solutions of a known Y concentration were loaded into the sample chamber using a microsyringe. The sample was compressed between the two diamond anvils only enough to seal the sample chamber. Pressure was increased after assembling the HDAC in the synchrotron hutch (Figure 2). Two thermocouples were used to measure temperature; one thermocouple on each side of the diamonds. The thermocouples were manufactured by Omega with a diameter of 0.003 inches and made of alumel-chromel, type K, whereas the heater wires were made of molybdenum (0.010 inches in diameter). Resbond 940, a zirconium-based cement, was used to hold the diamonds, thermocouples, heater wires, and gasket in place.

The HDACs were heated resistively by using three variable transformers. A main 20 ampere maximum transformer controlled two 10 ampere maximum transformers that were connected separately to each heater of the HDAC. This arrangement provides for flexible heating rates and fine temperature control. The temperatures in these experiments were maintained constantly to ±5 °C of the target temperatures. Argon-hydrogen (1% Hydrogen) gas was allowed to flow over the diamonds and the heaters to prevent corrosion during high-temperature operation. The temperature was elevated by increasing the amount of current sent through the heater wires by the variable transformers. The sample was first heated to about 75 °C to make sure the sample chamber had not failed under a small increase in temperature and that the heaters and thermocouples were functioning properly, and then proceeded to the desired temperature for that experiment. Heating rates were approximately 50 °C/min and were consistent for each experiment

Experiments were performed primarily at station 16 ID-D, High Pressure Collaborative Access Team (HPCAT, Figure 3), Advanced Photon Source, Argonne National Laboratory. Preliminary research was conducted at station 16 BM-B and at the wiggler beamline X17C, NSLS, but the X-ray photon flux was found to be too low to resolve geologically reasonable concentrations of Y. Moreover, at both X17C and 16 BM-D, the hutch configuration did not have adequate space to properly set up the heating variacs for HDAC. A detailed rendering of the experiment setup in 16 ID-D is provided in Figure 3. It was determined that having the sample mounted at a 10 degree angle to the detector, hence reducing the background from Rayleigh scattering of the diamond anvils which is strongly peaked around zero degrees, with two slits post-sample (slit openings of

1.0 by 0.5 mm and 0.2 by 0.3 mm for the first and second set of slits, respectively) resulted in the optimum signal-to-noise ratio. The slits did not completely remove the low intensity X-ray beam tails. A clean-up slit, or pinhole (50 μm diameter), was placed in the beam path directly before the HDAC to attempt to eliminate the low-intensity tails but this reduced the flux to a degree where our minimum detection limit was too adversely effected and, thus, could not be used. Amptek XR-100T-CZT (CdZnTe) and Vortex EX60 (Si-drift) detectors were used. The greatest difference between the two detectors is resolution and sensitivity where the Amptek and Vortex have resolutions of 146 and 136 eV, respectively. The Vortex detector was found to be more sensitive in this study. X-ray fluorescence (XRF) was used with an energy of 18.5 keV with the Amptek Detector and 20.0 keV with the Vortex detector to identify the Y in solution. The available energy range at 16 ID-D was from 16-21 keV. Yttrium was chosen as the element to use in this study because it is commonly used in conjunction with REE to characterize magmas (Sun and McDonough, 1989) and metamorphic geothermometers (Pyle et al., 2001). The elements Rb, Sr, Zr, and Nb were also considered, but the available energy range was deemed more suitable for Y. Specifically, the $K_{\alpha 1}$ emission line for Y is not above the operational energy range of beamline 16 ID –D (16-20 keV) (Table 1), and its K-edge is close to the range and would therefore be fluoresced.

Experimental Procedure

Experiments were initially performed at station 16 BM-D by equilibrating a synthetic monazite crystal and pure H_2O. After several unsuccessful attempts to resolve element energies with this assemblage, I concluded that a much more methodical approach was

needed at a beamline with much greater X-ray photon flux. These early studies also revealed the issue of parasitic fluorescence from the monazite sample which is excited by low intensity beamtails covering several 10s of micrometers in diameter beyond the full width half maximum (FWHM) of the primary beam. At station 16 ID-D we used a 1000 mg/L Y standard solution (Acros Organics #196455000; Y in H_2O/3% nitric acid) to make a standard working curve with concentrations of 1, 10, 50, 75, 100, 250, 500 and 750 mg/L. While the fluids being released during subduction are likely more complex (see Manning 2004 and references therein), these standards are appropriate for the development of this technique. A solution of each concentration was loaded separately into four-sided 4.5 mL VWR Polystyrene ($[C_8H_8]_n$) cuvettes (1.2 cm x 1.2 cm x 4.5 cm; catalog #89047-232). XRF spectra were collected of each serial dilution and the 1000 mg/L standard for 1200 seconds. Durations longer than 1200 seconds did not result in a spectrum that was improved in any respect and acquiring for a significantly lesser duration (<900 seconds) resulted in a spectrum where the background overwhelmed the Y signal. This procedure was then repeated using the HDAC instead of the cuvettes. The sample chamber was opened and thoroughly cleaned between the loadings of each solution.

Data Analysis

The signal from the detector was converted to a graphical user interface with the IDL (interface design language) MCA (multi-channel analyzer) program. This program saves the data in extensionless files which were then converted to ASCII files (<filename>.asc). These files were then opened with the Materials Data Incorporated (MDI) Jade software.

The background was first determined and removed. The peak profile was then fitted with a Gaussian function. This step calculates of the area beneath each identified peak. Jade calculates the area of peak as the sum of net intensities of data points greater than or equal to, and within the left and right background points (MDI Jade). If the uncertainties in the areas of the peaks generated by Rayleigh scattering were not within the uncertainty of each spectrum, then all peaks were normalized using the Rayleigh peak area to the 1000 mg/L spectrum. The peak generated by Rayleigh scattering is the most representative feature of the consistency of the incoming photons and, thus, is the best for normalizing data.

CHAPTER 3

RESULTS

Results from Station 16 BM-B

Initial experiments were performed at HPCAT using beamline 16 BM-B with monazite and gold in H_2O (Figure 4). I observed fluorescence signals of lanthanum (La, from monazite, $LaPO_4$), gold (pressure standard), rhenium (gasket), and germanium (detector). The signals were easily discerned from the background signal and the work looked promising. However, when the X-ray beam center was translated into the fluid only area of the sample chamber the X-ray fluorescence signal did not change. Even though a clean-up slit, or pinhole, was being used to remove the X-ray beam "tails", fluorescence from the solid phase was still observed.

While formulating a way to overcome the fluorescence of the solid phase without modification of the HDAC and diamond anvils, I developed a calibration curve for Y as I knew later in the experiments it would be used. Even at the concentration of our standard solution (1000 mg/L) I could not observe any fluorescence signal in a large volume (1-2 mL) or in the HDAC. Due to these circumstances it was decided to move to beamline 16 ID-D as that beamline provides more flexibility in the focusing of the X-ray beam and has a higher X-ray photon flux by approximately four orders of magnitude. It was thought that this increased flux would allow us to better observe fluorescence of elements in solution.

Results from Station 16 ID-D

Calibration in the Cuvettes

The spectrum of the 1000 mg/L Y standard solution contains three peaks (Figure 5). The peaks at 14.96 keV, 17.51 keV, and 18.50 keV are the fluorescence signal from Y, a peak resulting from Compton scattering of the incoming X-rays by diamond, and a peak resulting from elastic (Rayleigh) scattering of the incoming X-rays by diamond, respectively. The energy at which the peaks appear in some figures may differ owing to different detector calibrations. Changing the calibration was necessary when the detector was changed. Figure 6 shows the fit, and residuals of the fit, for the 1000 mg/L Y fluorescence peak and the peak due to the elastic scattering of the X-rays (see Table 2 for all calculated peak areas). All collected XRF spectra of the Y solutions show an increase in peak area with increasing Y concentration (Figures 7A and 7B for the Amptek and Vortex detectors, respectively). The spectrum from an empty polystyrene cuvette is included. There is no peak in that spectrum indicating that there is no contribution from the cuvette to the yttrium fluorescence peak. The relationship between peak area and concentration has been fit by a linear function (Figure 8). There are too few points in each data set to consider fitting with a more complicated function, thus, only a linear fit was considered.

Calibration in the HDAC

The spectra do not display the same behavior when each solution was loaded in the HDAC (Figure 9). It is not possible to distinguish a Y peak from the background signal when using the Amptek detector (Figure 9A). Additionally, the spectra in Figure 9A are indistinguishable from the spectrum of the empty HDAC. While this may indicate a lack

of fluid contained within the sample chamber, each load was verified by incrementally lowering the pressure until a small (<30 μm) vapor bubble was visible. The pressure was then increased slightly until the vapor bubble was no longer visible. When using the Vortex detector and a 1000 and 500 mg/L Y solution in the HDAC, a peak is observable (Figure 9B). Unfortunately, only the peak observed using the 500 mg/L Y solution was statistically sufficient to be fitted with the peak-fitting software. The spectrum of broad peak observed with the 1000 mg/L Y solution could not be distinguished from the background sufficiently to be fitted. With only one peak it is impossible to determine a peak area vs. concentration calibration curve with the HDAC in this setup.

CHAPTER 4

DISCUSSION

Cuvettes: Peak Area vs. Concentration

The relationship of peak area to concentration as it is observed in the cuvettes may be linear. The applied fits to the two datasets (Figure 8) display slopes of a different value; 190 and 723 for data gathered with the Amptek and Vortex detectors, respectively. The low concentration points (<500 mg/L) of the two sets correlate well, but at 500 mg/L the point recorded with the Vortex detector is significantly greater than that recorded by the Amptek detector (by 200+%). If the 500 mg/L point collected with the Vortex detector is considered an outlier, there are not enough points from that dataset to interpret a trend, but the low concentration points correlate well with the data from the Amptek detector. However, if the 500 mg/L point from the Vortex detector is not an outlier; the slope of the peak area vs. concentration curve varies with detector type. As experiments where the fluorescence of an element in solution is used to quantify concentration are beginning to be conducted more frequently this is a noteworthy observation. In future research it is pertinent to conduct a calibration study similar to that in this work prior to conducting experiments in order to lessen uncertainty in the procedures used to quantify concentration. Additionally, conditions vary at different beamlines, let alone different synchrotron facilities, thus, it is likely good practice to conduct a calibration study prior to each set of experiments.

HDAC Experiments

I was not able to reproduce the observations from the cuvettes in the HDAC. A broad peak was identified in the spectrum of the 1000 mg/L Y solution in the HDAC. However, it was not fitted by the peak-fitting software. Additionally, the scatter of the background and of the 1000 mg/L spectrum overlap; thus, any statement or calculation made regarding the 1000 mg/L spectrum would be questionable at best.

The peak obtained for the 500 mg/L solution was well above background and could be fitted. However, it is puzzling that the 1000 mg/l solution gave a very weak signal. A likely, yet incorrect, conclusion is that the 500 mg/L solution was mistakenly switched and in fact the largest observed peak is from the 1000 mg/L solution. However, extra care was taken to prevent these mistakes and the 1000 mg/L solution was reloaded in the HDAC (after cleaning the anvils and ultrasonically cleaning the gasket) and the result was no different. It is possible, but yet unverified, that when the 1000 mg/L solution was used there was precipitation of the Y along the walls of the gasket and thus, statistically significant Y fluorescence was observed. If there was precipitation from the 1000 mg/L solution, it is puzzling why a peak equal to or greater than that of the 500 mg/L solution is not observed due to Y that would have remained in solution. Given these data, it is clear that a significant refinement of the setup at 16 ID-D is required to further this technique at HPCAT. With only one data point based on a signal statistically sufficient for fitting a peak area there can be no meaningful trend or calibration curve calculated.

Given that the Vortex detector is more sensitive than the Amptek, this may explain why no Y fluorescence was observed with the Amptek detector (Figure 9). It is unlikely that the Amptek CdZnTe detector can be used for these experiments. However, Amptek

has more recently released CdTe, Si-Pin, and Si-Drift detectors that are more sensitive and may be suitable. Unfortunately, these detectors were not available for our use at APS.

Previous studies that have performed similar experiments with success (Schmidt et al., 2007; Manning et al., 2008; Sibert et al., 2008) used modified diamond anvils (drilled/recessed) to allow for a 90° orientation (detector at 90° to incoming beam path). These modified anvils are not capable of reaching pressures greater than 2 GPa, the P required to conduct experiments relevant to subduction zones and a multitude of other geologic conditions. Experiments can be conducted in a 90° orientation without modification of the anvils, but beryllium gaskets must be used. As beryllium is known to cause lung cancer and machining it would be necessary, this was not seen as a viable alternative regardless of any safety precautions (see Kolanz, 2001 and references therein). Without modification of the diamond anvils and other parts of the HDAC a solution is not apparent at this time. Some of these modifications would have been undertaken, however, they would have prevented us from conducting experiments at our target conditions (2–5 GPa and 600–850 °C). It is imperative that element partitioning at these conditions be studied as it is where the majority of dehydration is hypothesized to take place, and therefore the conditions where the generation of melt and element partition is the most likely to occur. Also of importance is the reduction of parasitic fluorescence from the interaction of low-intensity X-ray beam tails that may be present. This can produce peaks that may be thought to be generated by the sample, when they are caused by an object in the beam path and/or part of the HDAC.

CHAPTER 5

CONCLUSIONS

This work set out to complement current techniques (piston-cylinder, multi-anvil, HDAC with modified anvils) for quantifying element mass transfer between a solid and fluid phase or phases. I have determined that at 16 ID-D at HPCAT, APS, ANL the relationship between the peak area of yttrium fluorescence and the concentration is likely linear. This was determined in cuvettes and could not be reproduced in the hydrothermal diamond anvil cell. At this time, a solution to these issues is not present. If the obstacles preventing this technique from generating reproducible data in the HDAC could be overcome, these experiments would fit a niche in temperature-pressure conditions which are higher than many researchers use for piston cylinder experiments, and lower than many use for multi-anvil experiments. The hydrothermal diamond anvil cell is also considerably less expensive alternative to a piston cylinder or multi-anvil apparatus.

Table 1. X-ray fluorescence emission energies ($K_{\alpha 1}$) of elements considered in this study.

Element	Energy
Rb	13.39
Sr	14.16
Y	14.96
Zr	15.77
Nb	16.61

Table 2. Areas and 1-σ uncertainties (in parentheses) in the fit of the area of the Y peak, and the peak generated by Rayleigh scattering, for each solution and detector type used. ND = No Data; ? = uncertainty could not be calculated.

Vessel	Detector Type	Concentration in mg/L	Y Area	Rayleigh Area
Cuvettes	Amptek XR-100-CZT	10	9999 (512)	103068 (2068)
		75	25992 (530)	107796 (1930)
		100	33848 (1361)	108547 (2326)
		250	71783 (1433)	109364 (2022)
		500	110753 (2042)	108431 (1925)
		750	139120 (1177)	112036 (2020)
		1000	211987 (2421)	106063 (2102)
	Vortex EX60	50	5496 (322)	416385 (3343)
		250	65889 (2020)	416505 (3339)
		500	324905 (5085)	426265 (3620)
HDAC	Amptek XR-100-CZT	10	ND	21240 (759)
		100	ND	22294 (840)
		500	ND	29268 (655)
	Vortex EX60	100	ND	48904 (895)
		500	3383 (150)	46231 (913)
		1000	105 (?)	110572 (1459)

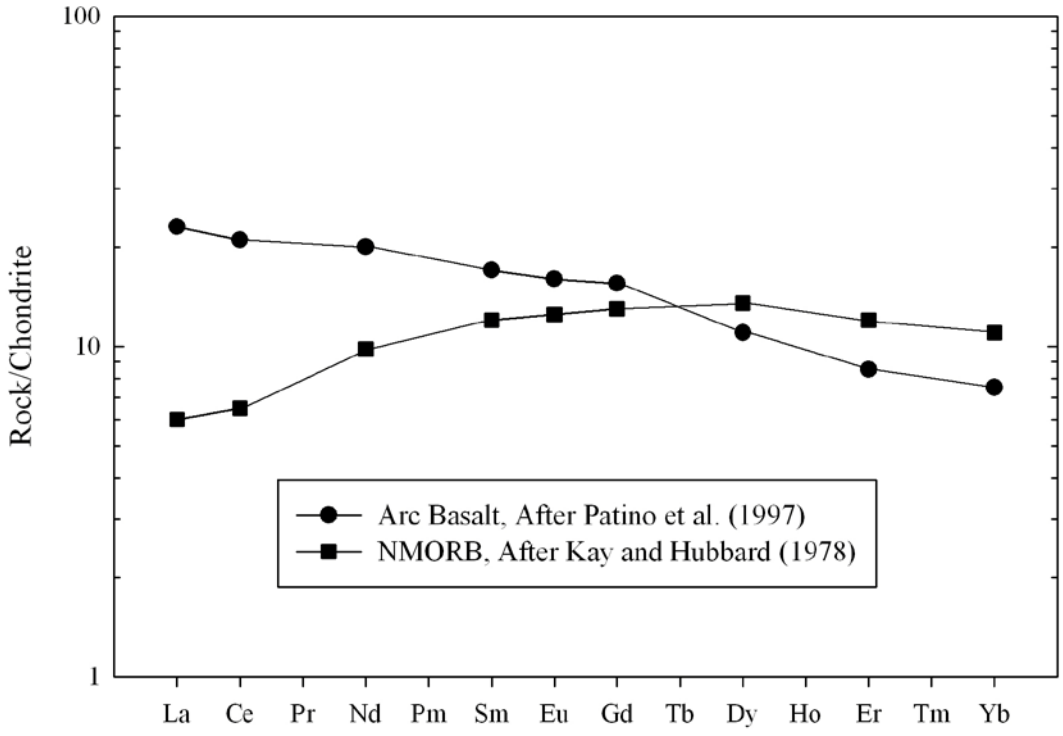

Figure 1. Island arc chondrite normalized "spider" diagrams after Patino et al. (1997, Honduras) and Kay and Hubbard (1978, various mid-ocean ridges). Theses analyses of rock(s) gathered at or near the surface of volcanic arcs are often used to discern processes occurring at the mantle-wedge interface.

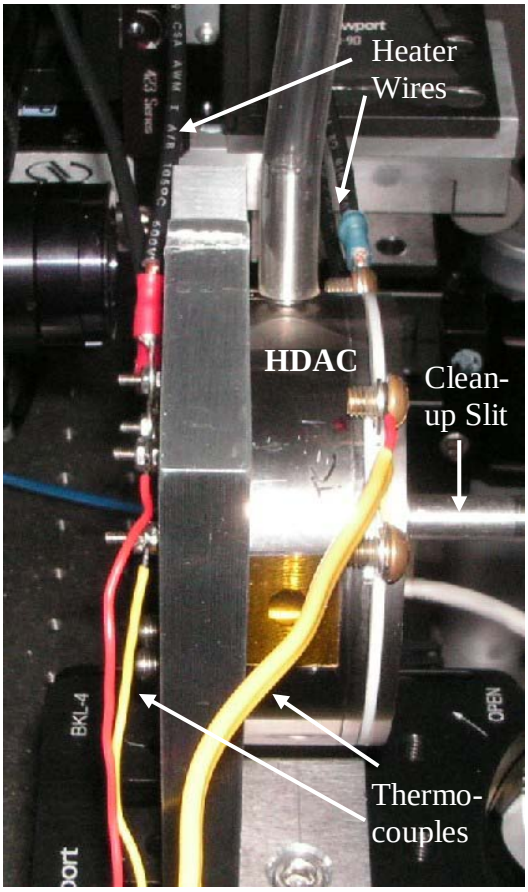

Figure 2. The Hydrothermal Diamond Anvil Cell has a heater surrounding each diamond and thermocouples touching the surface of each diamond. The tube (top) supplied Argon (1% Hydrogen) gas. The clean-up slit is on the right side of the picture.

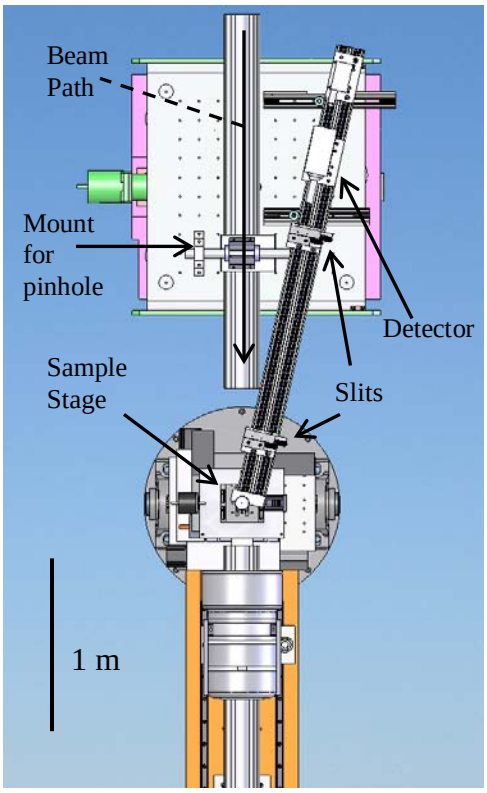

Figure 3. The experimental setup at 16 ID-D features a semi-backscatter orientation with the slits and detector at a 15° angle to the incoming beam. The location of the detector, slits, sample stage and the X-ray beam path are noted in the figure. The HDAC was rotated 10° (clockwise when looking at this figure) during these experiments.

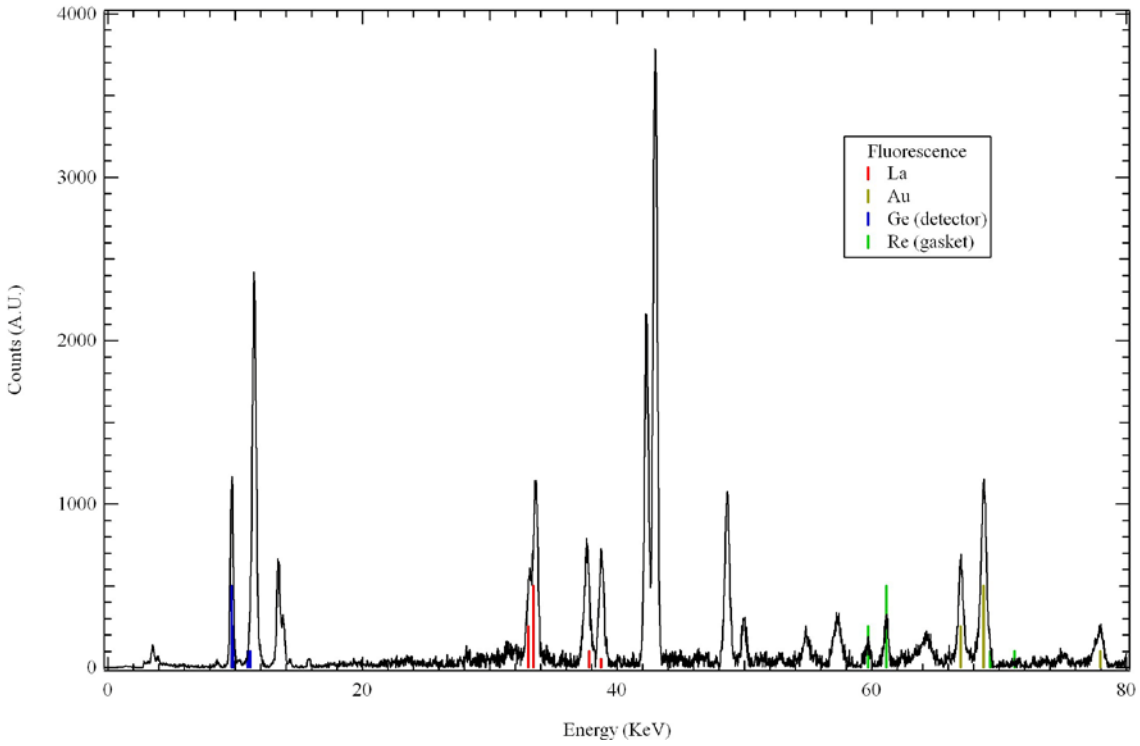

Figure 4. X-ray fluorescence experiments performed at APS beamline 16 BM-B resulted in the realization that parasitic fluorescence from a solid phase was a significant obstacle to refining this technique. The spectrum above shows X-ray fluorescence and diffraction peaks of gold (pressure standard), rhenium (gasket), germanium (detector), and lanthanum (in the mineral monazite, $LaPO_4$). Only fluorescence peaks are highlighted with colored lines. When the center of the X-ray beam was moved onto the fluid in the sample chamber the same X-ray fluorescence spectrum was observed. Thus, La fluorescence from the solid phase (monazite) was contaminating the signal that was thought to be generated by fluorescing La in the fluid.

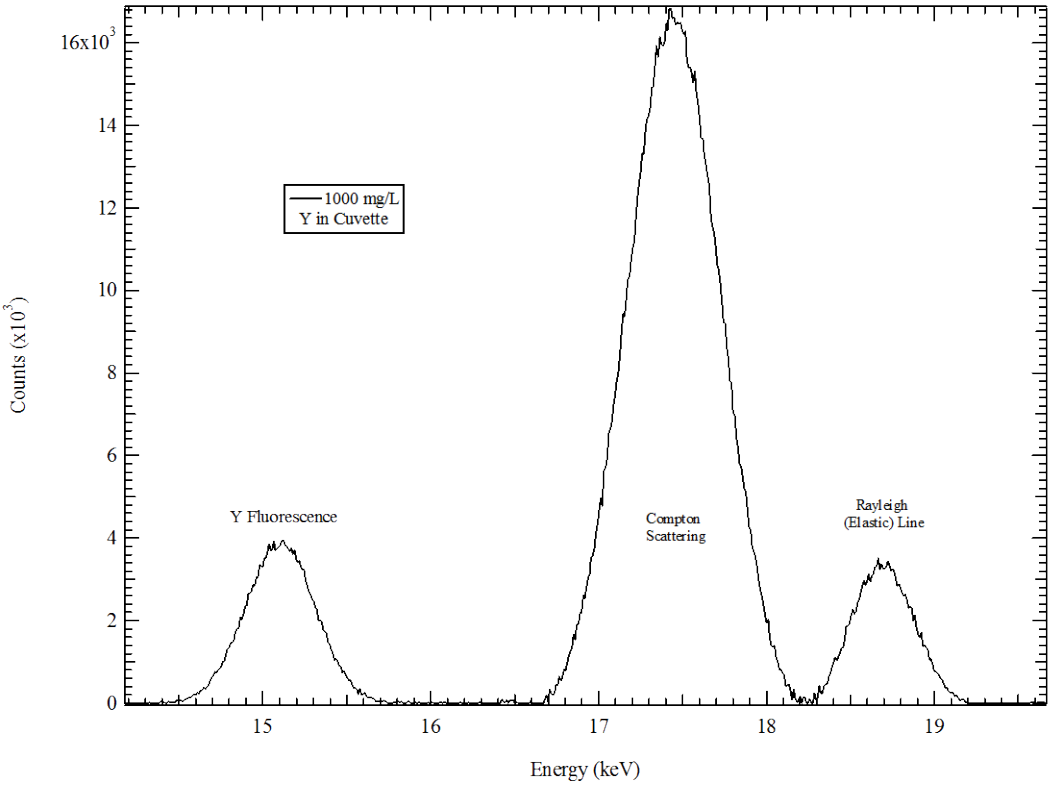

Figure 5. The XRF spectrum for the Y 1000 mg/L solution contains three peaks which are the Y fluorescence (14.96 keV), Compton scattering (17.51 keV), and Rayleigh (elastic) scattering (18.5 keV).

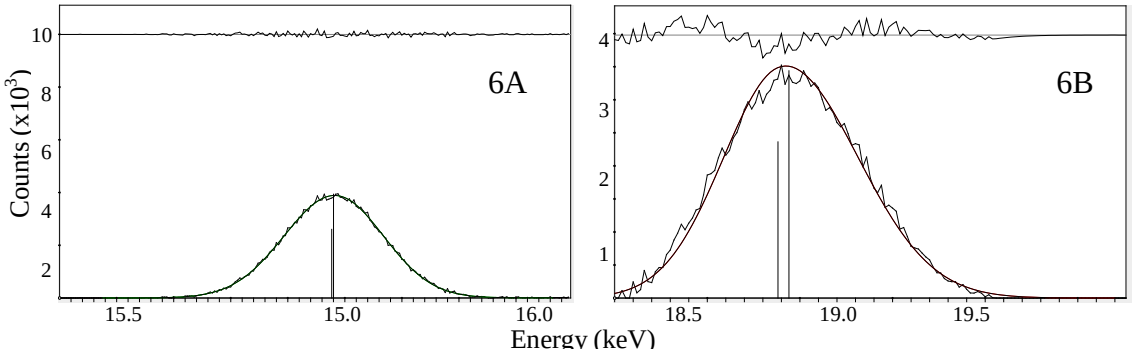

Figure 6. Y fluorescence peak from the 1000 mg/L solution fitted with a Gaussian function (smooth line, 6A). The residuals of the fit are represented by the line at the top of the figure. The calculated peak area was 211987 ± 2421 (arbitrary units, 1-σ uncertainty). The peak resulting from Rayleigh (elastic) scattering was also fit with a Gaussian function (6B). The resulting residuals of the fit are represented by the line at the op of the figure. The calculated peak area was 106063 ± 2102 (arbitrary units, 1-σ uncertainty). The process for these fits was repeated for the spectra of each concentration.

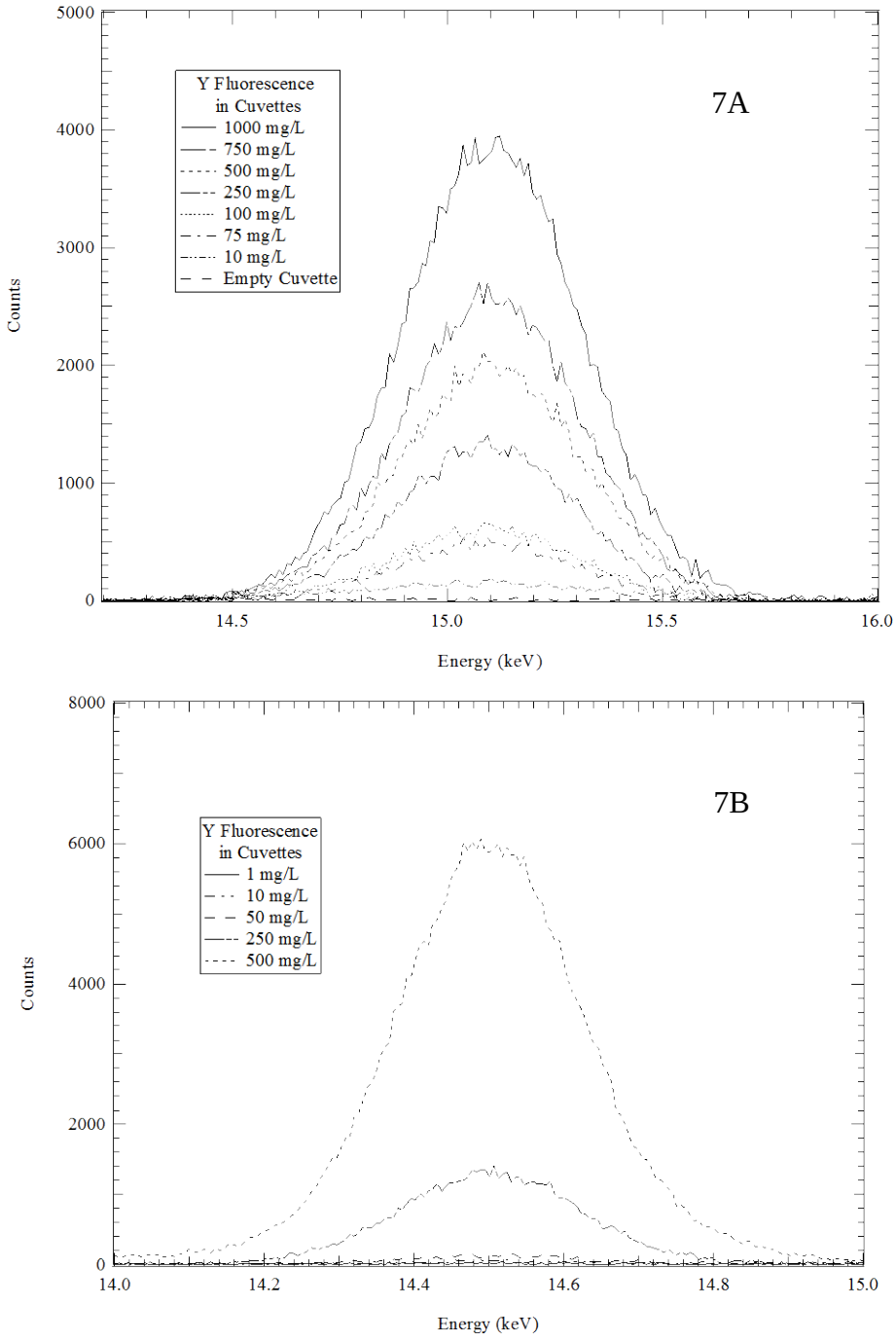

Figure 7. The area of the Y fluorescence peak increases with increasing concentration. The spectrum of an empty cuvette can be observed below the 10 mg/L spectrum (7A). The spectra in Figure 7A were recorded with an Amptek XR-100 CZT detector whereas the spectra in Figure 7B were recorded with a Vortex EX60 detector.

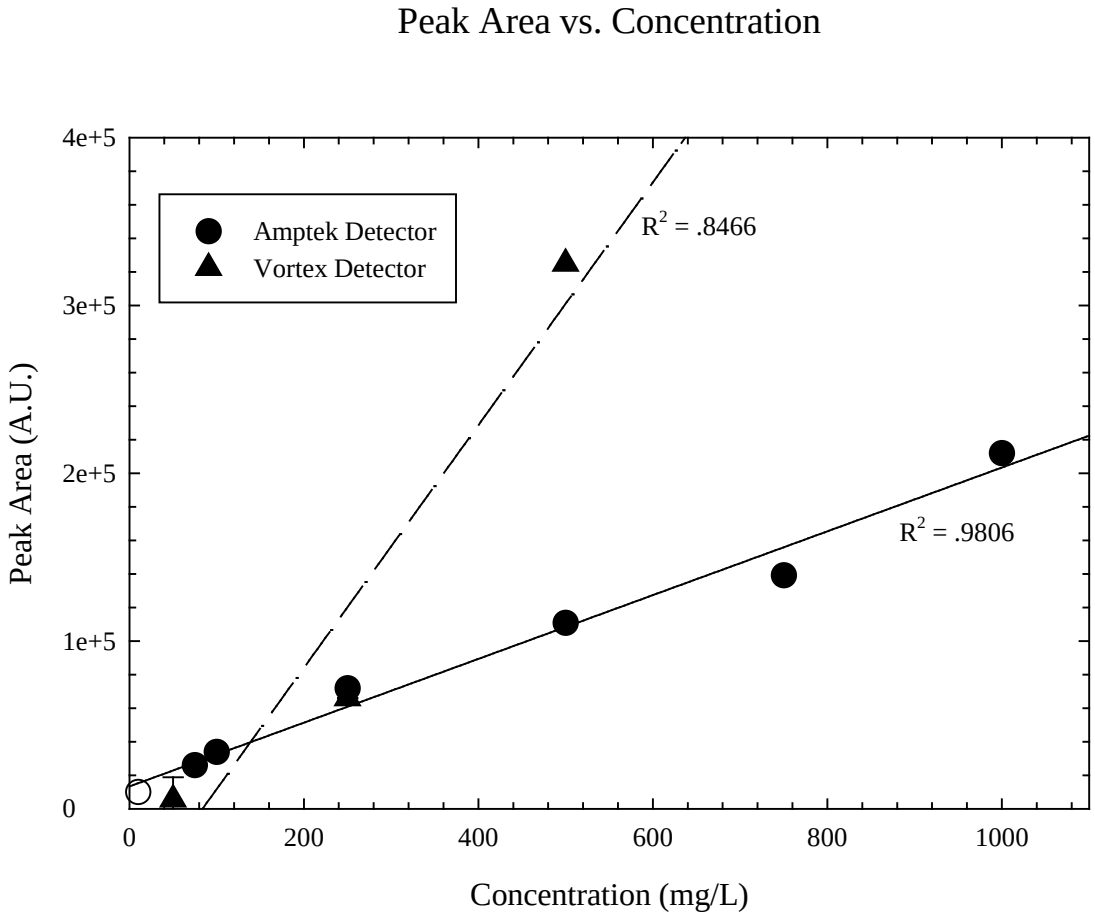

Figure 8. The peak area for the cuvette was plotted versus concentration. A linear function was fit to the data ($y = y_0 + ax$). For the Vortex detector fit y_0 = -60748.4919, a = 723.1693, and R^2 = 0.8466 (three points); and for the Amptek detector fit y_0 = 13312.5564, a = 190.0537, and R^2 = 0.9806 (seven points). The 1-σ uncertainty in the peak area for all points is within the size of the symbols (see Table 2 for values).

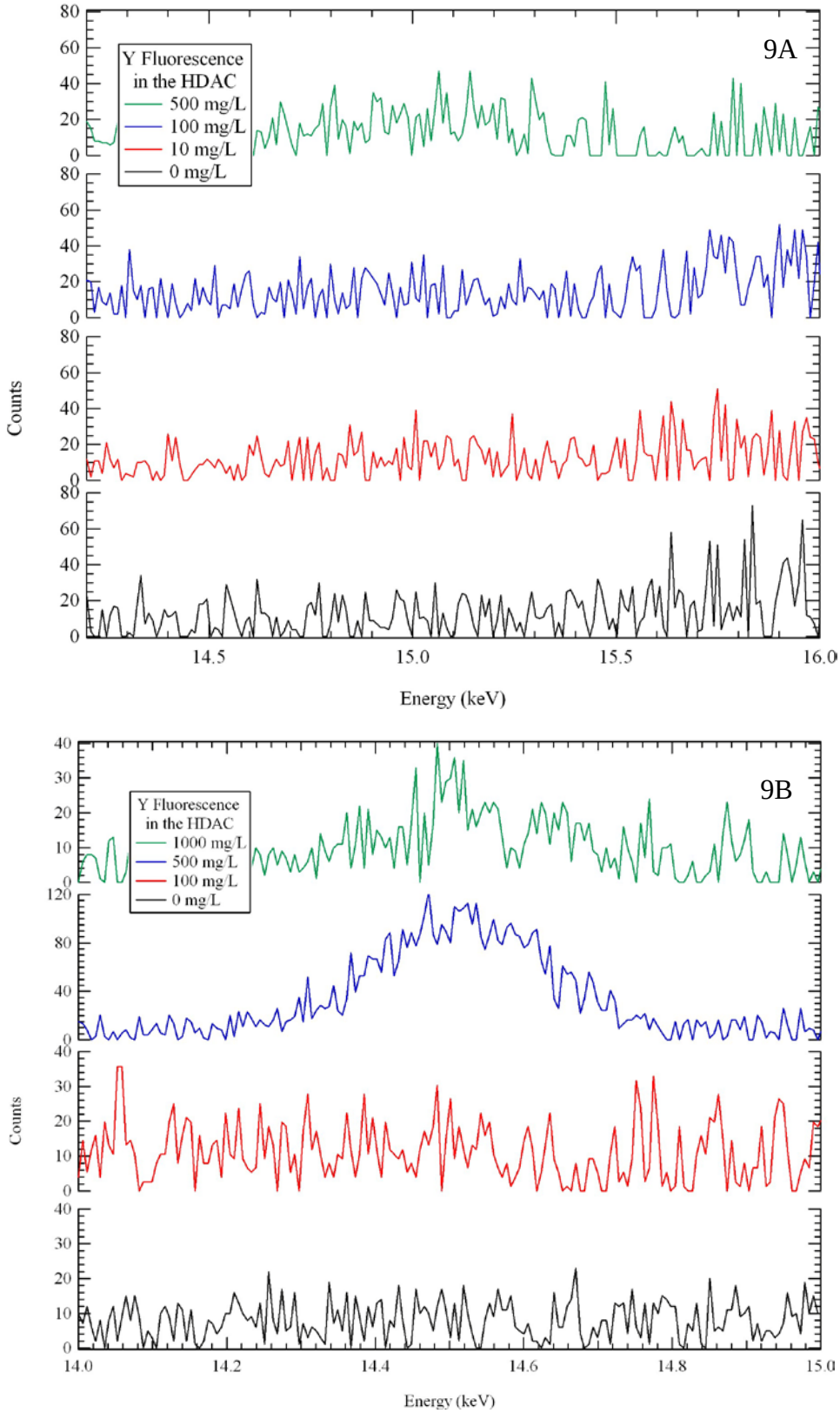

Figure 9. The Y fluorescence peak from the 500 mg/L solution is observed from within

the HDAC. However, it is not possible to distinguish Y fluorescence (14.96 keV, shown at ~15.1 and 14.5 keV in 9A and 9B, respectively; the shift is due to detector calibration) of 100 or 1000 mg/L from the background signal when each solution was loaded into the HDAC. The spectra in Figure 9A were recorded with an Amptek XR-100 CZT detector whereas the spectra in Figure 9B were recorded with a Vortex EX60 detector.

REFERENCES

Ayers, J., and E.B. Watson, 1991, Solubility of apatite, monazite, zircon, and rutile in supercritical aqueous fluids with implications for subduction zone geochemistry, *Phil. Trans.: Phys. Sci. Eng.*, **335(**1638), 365-375.

Bassett, W.A., Shen, A.H., Bucknum, M., and I-M. Chou, 1993, A new diamond anvil cell for hydrothermal studies to 2.5 GPa and from – 190 to 1200 °C, *Rev. Sci. Instrum.*, **64**(8), 2340-2345.

Bassett, W.A., 2003, High pressure-temperature aqueous systems in the hydrothermal diamond anvil cell (HDAC), *Eur. J. Mineral.*, **15**, 773-780.

Beate, B., Monzier, M., Spikings, R., Cotton, J., Silva, José, Bourdon, Erwan, and J-P. Eissen, 2001, Mio–Pliocene adakite generation related to flat subduction in southern Ecuador: the Quimsacocha volcanic center, **192**, 561-570.

Chan, L.H., Leeman, W.P. and C.-F. You, Lithium isotopic composition of Central American Volcanic Arc lavas: implications for modification of subarc mantle by slab-derived fluids, *Chem. Geol.*, **160**, 255-280.

Elliot, T., 2003, Tracers of the slab, in *Inside the Subduction Factory*, J. Eiler (ed.), Geophysical Monograph **138**, 23-45.

Ewart, A., Collerson, K.D., Regelous, M., Wendt, J.I., and Y. Niu, Geochemical Evolution within the Tonga–Kermadec–Lau Arc–Back-arc Systems: the Role of Varying Mantle Wedge Composition in Space and Time, *J. Petrol.*, **39**, 331-368.

Grove, T. L., Chatterjee, N., Parman, S.W., and E. Médard, 2006, The influence of H_2O on mantle wedge melting, *Earth Plan. Sci. Lett.*, **249**, 74-89.

Hermann, J., and C.J. Spandler, 2008, Sediment melts at sub-arc depths: an experimental study, *J. Pet.*, **49**(4), 717-740.

Hawkesworth, C.J., Gallagher, K., Hergt, J.M., and F. McDermott, 1993, Mantle and slab contributions in arc magmas, *Annu. Rev. Earth Planet. Sci.*, **21**, 175-204.

Iwamori, H., 1998, Transportation of H_2O and melting in subduction zones, *Earth Plan. Sci. Lett.*, **160**, 65-80.

Iwamori, H., 2004, Phase relations of peridotites under H_2O-saturated conditions and ability of subducting plates for transportation of H_2O.

Johnson, M.C, and T. Plank, 1999, Dehydration and melting experiments constrain the fate of subducted sediments, *Geochem. Geophys. Geosys.*, **1**(1), doi:10.1029/1999GC000014.

Kawamoto, T., 2006, Hydrous phases and water transport in the subducting slab, *Rev. Min. Geochem.,* **62**, 283-289.

Kay, R.W., 1978, Aleutian magnesian andesites: Melts from subducted Pacific ocean crust, *J. Volcan. Geotherm.*, **4**, 117-132.

Kay, R.W. and N.J. Hubbard, 1978, Trace elements in ocean ridge basalts, *Earth Plan. Sci. Lett.*, **38**, 95-116.

Keppler, H., 1996, Constraints from partitioning experiments on the composition of subduction-zone fluids, *Nature,* **380**, 237-240.

Kessel, R., Schmidt, M.W., Ulmer, P., and T. Pettke, 2005, Trace element signature of subduction zone fluids, melts, and supercritical liquids at 120-180 km depth, *Nature,* **437**(7059), 724-727.

Kessel, R., Ulmer, P., Pettke, T., Schmidt, M.W., and A.B. Thompson, 2004, A novel approach to determine high-pressure high-temperature fluid and melt compositions using diamond-trap experiments, *Am. Min.,* **89**(7), 1078-1086.

Klemme, S., Prowatke, S., Hametner, K., and D. Günther, 2005, Partitioning of trace elements between rutile and silicate melts: Implications for subduction zones, *Geochem. Cosmochem. Acta,* **69**(9), 2361-2371.

Kolanz, M.E., 2001, Introduction to beryllium: Uses, regulatory history, and disease, *App. Occu. Environ. Hygiene*, **16**(5), 559-567.

Manning, C.E., 2004, The chemistry of subduction zone fluids, *Earth Plan. Sci. Lett.*, **223**, 1-16.

Manning, C.E., Wilke, M., Schmidt, C., and J. Cauzid, 2008, Rutile solubility in albite-H_2O and $Na_2Si_3O_7$-H_2O at high temperatures and pressures by in-situ synchrotron radiation micro-XRF, *Earth Plan. Sci. Lett.*, **272**, 730-737.

Moriguti, T. and E. Nakamura, 1998, Across-arc variation of Li isotopes in lavas and implications crust/mantle recycling at subduction zones, *Earth Plan. Sci. Lett.,* **163**, 167-174.

Patino, L.C., Carr, M.J., and M.D. Feigenson, 1997, Cross-arc variations in volcanic fields in Honduras, C.A.: progressive changes in source with distance from the volcanic front, *Contrib. Mineral. Petrol.,* **129**, 341-351.

Plank, T, and C.H. Langmuir, 1998, The chemical composition of subducting sediment and its consequences for the crust and mantle, *Chem. Geol.,* **145**, 325-394.

Plank, T., 2005, Cons**t**rain**t**s from **T**horium/Lan**t**hanum on Sedimen**t** Recycling a**t** Subduc**t**ion Zones and **t**he Evolu**t**ion of **t**he Con**t**inen**t**s, *J. Petrol.*, **46**, 921-944.

Prowatke, S., and S. Klemme, 2006, Trace element partitioning between apatite and silicate melts, *Geochem. Cosmochem. Acta,* **70**, 4513-4527.

Pyle, J.M., Spear, F.S., Rudnick, R.L., and W.F. McDonough, Monazite-xenotime-garnet equilibrium in metapelites and new monazite-garnet thermometer, *J. Pet.*, **42**(11), 2083-2107.

Reed, M.J., Candela, P.A., and P.M. Piccoli, 2000, The distribution of rare earth elements between monzogranitic melt and the aqueous volatile phase in experimental investigations at 800 °C and 200 MPa, *Contrib. Mineral. Petrol.*, **140**, 251-262.

Sanchez-Valle, C., Martinez, I., Daniel, I., Philippot, P., Bohic, S., and S. Simionovici, 2003, Dissolution of strontianite at high P-T conditions: An in-situ synchrotron X-ray fluorescence study, *Am. Min.*, **88**, 978-985.

Schmidt, C., Rickers, K., Bilderback, D.H., and R. Huang, 2007, In situ synchrotron-radiation XRF study of REE phosphate dissolution in aqueous fluids to 800 °C, *Lithos*, **95**, 87-102.

Schmidt, M.W. and S. Poli, 1998, Experimentally based water budgets for dehydrating slabs and consequences for arc magma generation, *Earth Plan. Sci. Lett.*, **163**, 361-379.

Sibert, J., Foy, E., Somogyi, A., Munsch, P., Simon, G., and S. Kubsky, 2008, In situ experimental study of subduction zone fluids using diamond anvil cells, *Eos Trans. AGU, 89*(53), Fall Meet. Suppl., Abstract U53A-0053.

Spandler, C.J., Mavrogenes, J., and J. Hermann, 2007, Experimental constraints and element mobility from subducted sediments using high-P synthetic fluid/melt inclusions, *Earth Plan. Sci. Lett.*, **239**, 228-249.

Sun, S.S and W.F. McDonough, 1989, Chemical and isotopic systematics of oceanic basalts: implications for mantle composition and processes, in *Magmatism in the Ocean Basins,* Saunders, A.D. and M.J. Norry (eds.), Geological Society Special Publication, **42**, 313-345.

Zack, T., and T. John, 2007, An evaluation of reactive fluid flow and trace element mobility in subducting slabs, *Chem. Geol.*, **239**, 199-216.

VITA

Graduate College
University of Nevada, Las Vegas

Steven Joseph Maglio

Degrees:

Bachelor of Science, Geology, 2005
Northern Illinois University

Master of Science, Geology, 2007
Northern Illinois University

Thesis Title: In situ element quantification in the hydrothermal diamond anvil cell using synchrotron X-ray fluorescence with applications toward subduction zone processes

Thesis Examination Committee:

Chairperson, Adam Simon, Ph.D.
Committee Member, Oliver Tschauner, Ph.D.
Committee Member, Eugene Smith, Ph.D.
Graduate Faculty Representative, Andrew Cornelius, Ph.D.